Comparison of body rotations using Euler angles and quaternions

Author:

Hendrik D Mouton [a]

Abstract:

Many comparisons between Euler angle and quaternion representations of body rotations have been done in the past, but what are additionally investigated in this article are the handling of the generally important non-zero starting conditions, and a demonstration of the correctness of the Euler to quaternion and quaternion to Euler conversions despite giving remarkably different Euler angle and quaternion values for the same set of starting values. Two Euler configurations are also investigated and compared to demonstrate that the findings are generally valid. The first is the often-used yaw-pitch-roll (inner) and the second the less known roll-yaw-pitch (inner) configuration. Some of the test scenarios were chosen such that both the Euler angle configurations had to move through their gimbal lock positions. All transformation matrices, using two sets of Euler angles, and three sets of quaternion values, gave the same projections in an inertial axes system of a point fixed to the rotating body doing a chosen set of rotations, but there are accuracy differences. Therefore there is an optimal solution for each Euler configuration. The findings of this paper are also important in tracking loops where these types of transformations are used in the relative geometry calculations where the angles, for example, between the target and the camera sightline, must be determined accurately.

Introduction:

Testing of all the configurations and transformation methods was done by the same procedure. A point on the body was specified (x_T, y_T, z_T), then 3 initial Euler angles were specified, then a chosen set of base motions was applied to the body, and lastly the projection path (X_T, Y_T, Z_T) in an inertial axes system of the specified point was calculated by simulation. The base motions $(\omega_{xb}, \omega_{yb}, \omega_{zb})$ were applied sequentially so that the effect of each can be distinguished in the results.

The two block diagrams below (Figures 1 and 6) show the two Euler configurations considered, and how the Euler angle transformation and quaternion transformation were done. One more Euler angle set, and two more quaternion sets were specified and evaluated for each configuration. The purpose of these extra transformations was to determine the accuracy of the Euler angle to quaternion and inverse conversions. All these transformations proved that the method is very robust, but some implementations are superior regarding accuracy. This will be determined and demonstrated below.

[a] Emeritus Associate Professor Hendrik D Mouton, Mechanical Engineering, University of Cape Town, Rondebosch 7701, Cape Town, South Africa, hennie.mouton@uct.ac.za

ψ, θ, ϕ (inner) Euler configuration and quaternions:

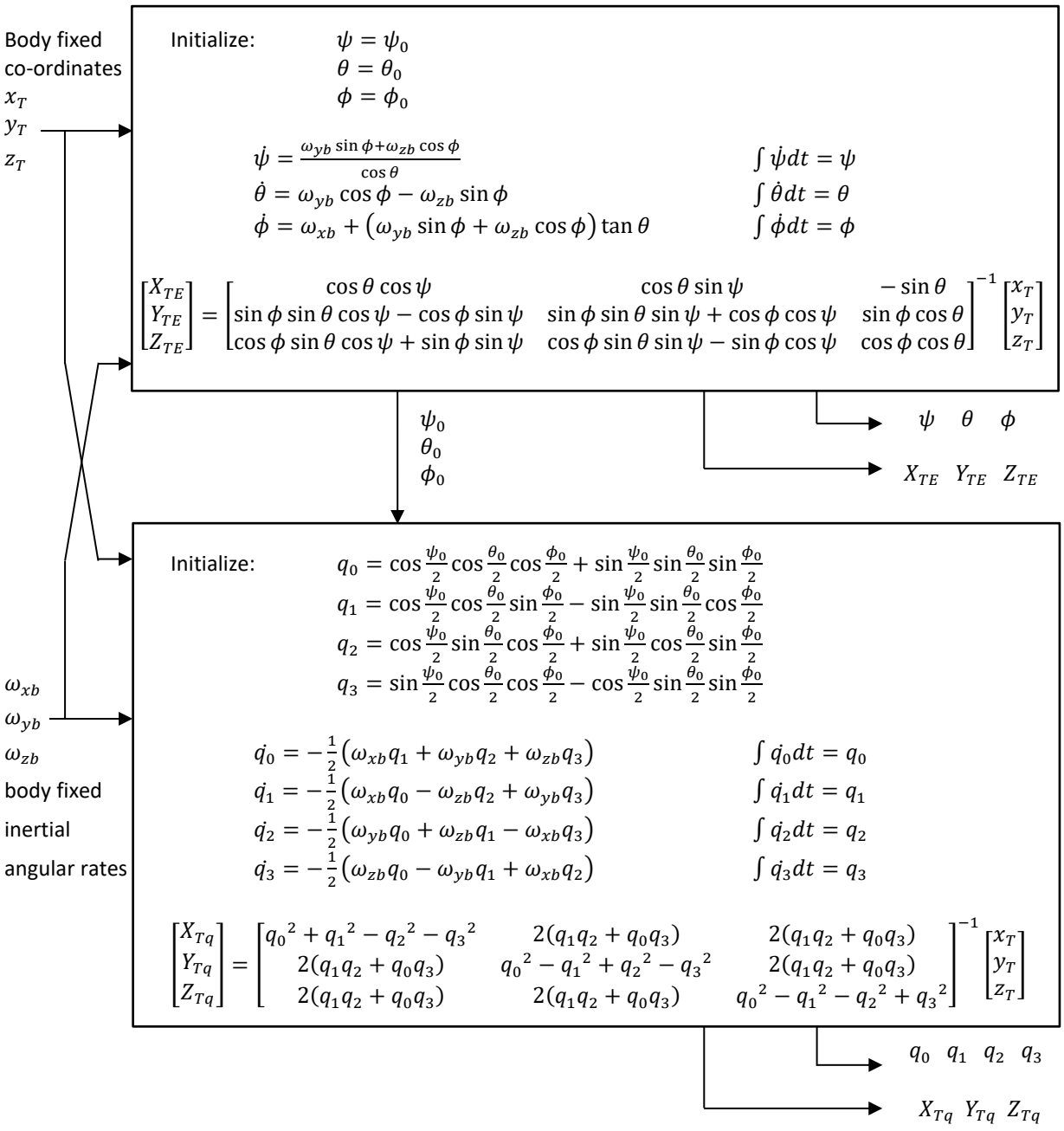

Figure 1. ψ, θ, ϕ (inner) Euler configuration and Quaternion block diagram

The quaternion values are normalised by dividing each value with $\sqrt{{q_0}^2 + {q_1}^2 + {q_2}^2 + {q_3}^2}$ after determining the integrals.

In this configuration Euler angles can be derived from quaternions with the following:

- $\theta_q = \text{asin}[2(q_0q_2 - q_1q_3)]$
- $\psi_q = \text{atan2}\left[\frac{2(q_1q_2 + q_0q_3)/\cos\theta_q}{({q_0}^2 + {q_1}^2 - {q_2}^2 - {q_3}^2)/\cos\theta_q}\right]$
- $\phi_q = \text{atan2}\left[\frac{2(q_2q_3 + q_0q_1)/\cos\theta_q}{({q_0}^2 - {q_1}^2 - {q_2}^2 + {q_3}^2)/\cos\theta_q}\right]$

Although divisions by $\cos\theta_q$, as in the last two equations, if negative, causes a 180° difference in the answer, it does not affect the transformation. These divisions may therefore be omitted. These calculated angles may differ from the Euler angles determined through simulation as shown in the top half of the block diagram, but the transformation will still produce the same results. The reason is that the angles will differ such that the components of the transformation matrix, consisting of products depending on the angle values, will stay the same. The ψ_q, θ_q, ϕ_q angles were used to determine a 2nd Euler transformation matrix.

By using the initializing equations for quaternions in the block diagram, two new sets of quaternions were calculated from ψ, θ, ϕ and ψ_q, θ_q, ϕ_q namely $q_{00}, q_{01}, q_{02}, q_{03}$ and $q_{000}, q_{001}, q_{002}, q_{003}$ respectively. These were used to determine 2nd and 3rd quaternion transformation matrices.

The simulation results follow.

Initial settings:

- $x_T = 0.8$ m, $y_T = 0.3$ m, $z_T = -0.2$ m
- $\psi = 0.4$ rad, $\theta = -0.4$ rad, $\phi = 0.0$ rad (must be set to 0.0 for θ to travel through 90°, a gimbal lock position chosen to be investigated)

Base motions of $2\pi 2.0$ rad/s constant rotational rates were applied as can be seen in the 1st set of 3 graphs in Figure2. The 3 Euler angles, mostly ramps, follow thereafter, followed by the Euler angles derived from the quaternions. Then follow the 3 sets of quaternions, drawn on slightly different scales (±1, ±1.1, ±1.2) so that they do not cover one another in the time slots where they are the same. Lastly the inertial co-ordinates of the chosen point in the body are drawn, the 1st set (X_{Tq}, Y_{Tq}, Z_{Tq}) by using the original quaternions for the transformation, and the 2nd set (X_{TE}, Y_{TE}, Z_{TE}) by using the original Euler angles for the transformation. These two sets are quite the same over the time drawn. No problems were experienced when θ went through the 90° gimbal lock position because the coding of the simulations was done such that the exact singularity point was avoided.

PTP in the titles of the graphs below denotes the Psi-Theta-Phi Euler configuration. Later the same investigations were done with the Phi-Psi-Theta Euler configuration.

Note the difference in θ and θ_q in Figure 2, as well as the differences in the same q-parameters. Despite of these differences (X_{Tq}, Y_{Tq}, Z_{Tq}) and (X_{TE}, Y_{TE}, Z_{TE}) are quite the same.

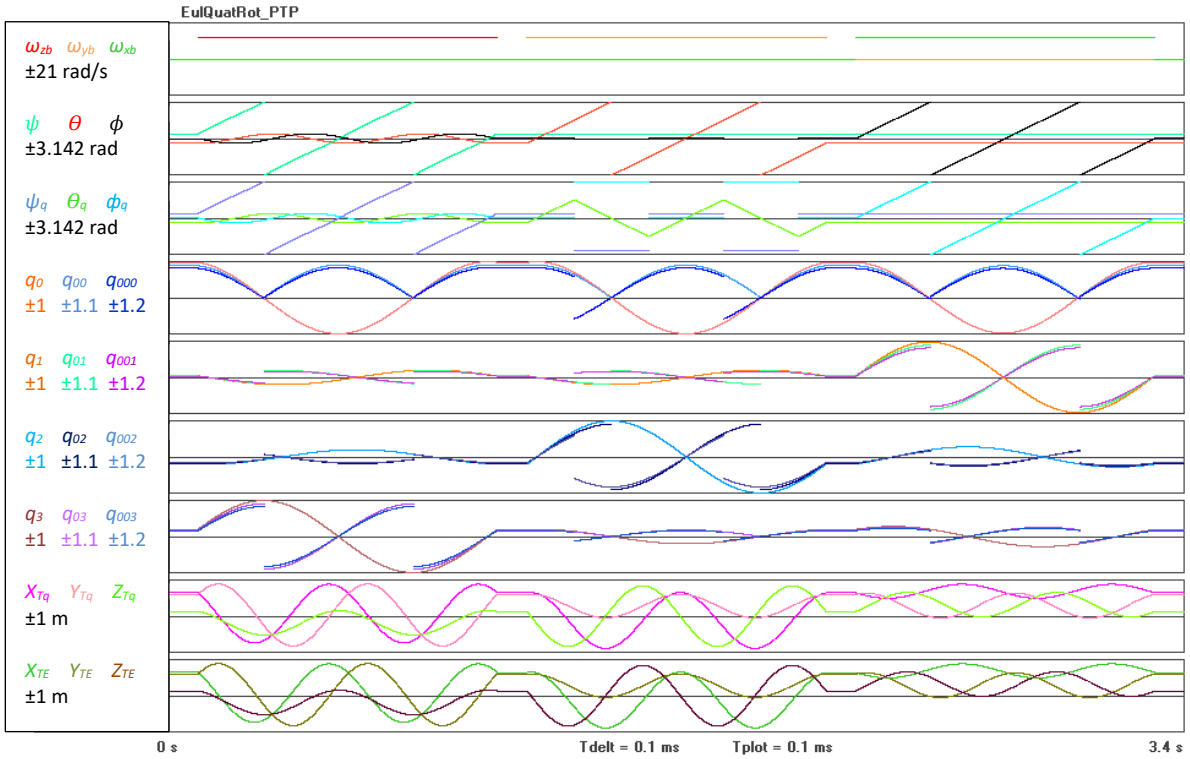

Figure 2. ψ, θ, ϕ configuration with initial $\phi = 0.0$ graphs

The next simulation was done similar to the previous one, except that the initial ϕ was changed from 0.0 to 0.1 rad. The changes in ψ, θ and ϕ are noteworthy compared to the previous graphs, but the general results are the same as before. The two sets of inertial co-ordinates are still quite the same. Compare (X_{TE}, Y_{TE}, Z_{TE}) in Figures 2 and 3.

Note the differences in the same q-parameters in Figure 3. Despite of these differences (X_{Tq}, Y_{Tq}, Z_{Tq}) and (X_{TE}, Y_{TE}, Z_{TE}) are quite the same.

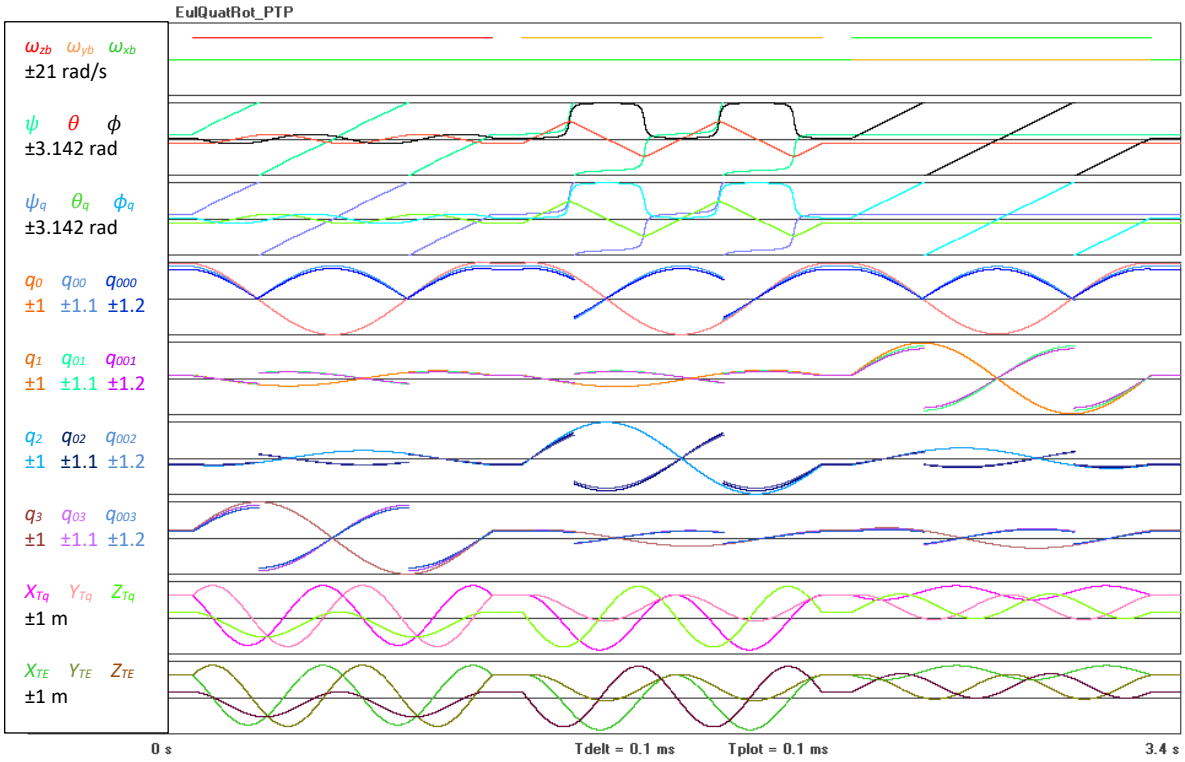

Figure 3. ψ, θ, ϕ configuration with initial $\phi = 0.1$ graphs

The set-up for the next two graphs is the same as the previous simulation; only different signals are plotted. Although the two sets of inertial co-ordinates appeared to be the same before, when plotting their differences on a more sensitive scale, it can be seen that they differ. These differences were also plotted for the transformations done with the other Euler angles and quaternions.

X_{Tq}, Y_{Tq}, Z_{Tq} are the co-ordinates, transformed with the quaternion matrix from quaternion equations.

X_{TE}, Y_{TE}, Z_{TE} are the co-ordinates, transformed with the Euler matrix from the gimbal equations.

X_{TEq}, Y_{TEq}, Z_{TEq} are the co-ordinates, transformed with the Euler matrix derived from quaternion equations.

X_{TqE}, Y_{TqE}, Z_{TqE} are the co-ordinates, transformed with the quaternion matrix derived from the gimbal equations.

X_{TqEq}, Y_{TqEq}, Z_{TqEq} are the co-ordinates, transformed with the quaternion matrix derived from Euler angles derived from quaternion equations.

In the next graphs it is clear that the transformations based on the Euler equations, are not very accurate. They are the 2nd and 4th sets of 3 graphs in Figure 4. It can be solved by performing the simulation at a much smaller incremental time step, which is not necessary for the transformations based on the original quaternions.

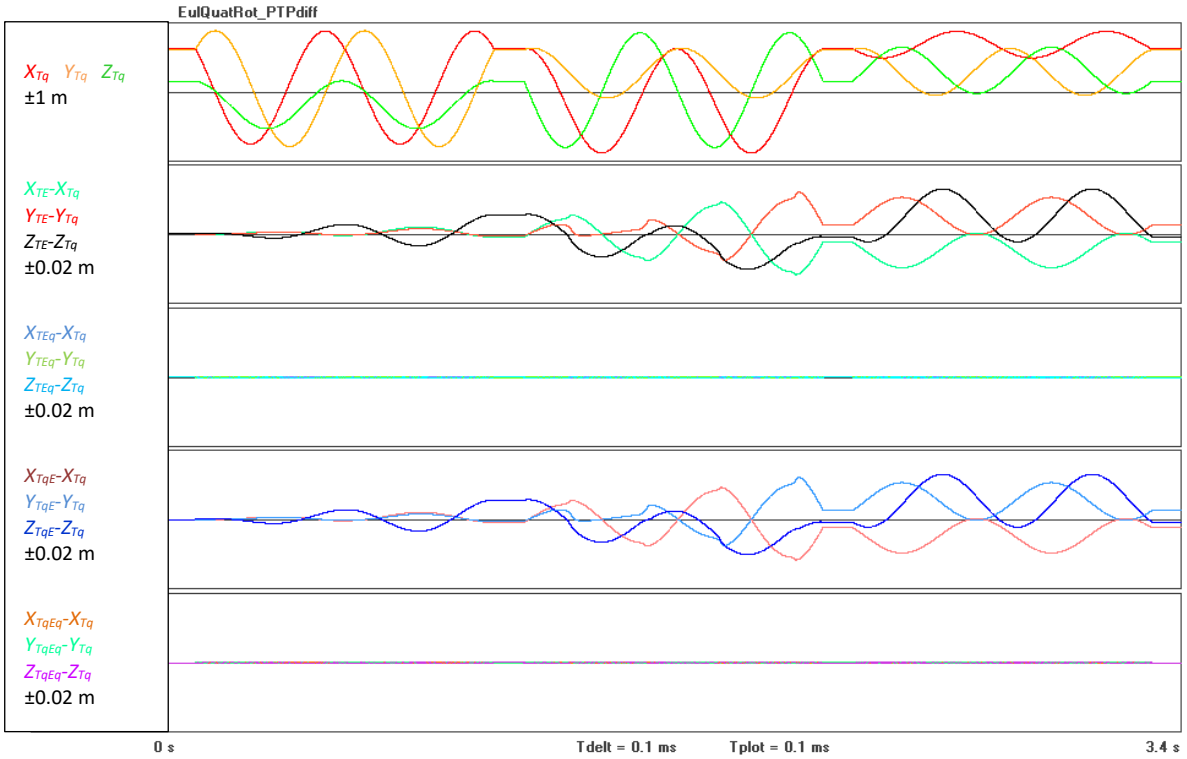

Figure 4. ψ, θ, ϕ configuration with time step = 0.1 ms graphs

Figure 5 shows that a 10 times smaller incremental time step improves the transformations based on the gimbal equations significantly, but a smaller time step is not required for transformations based on the original quaternions. This is strong indication that transformations based on quaternions are preferable.

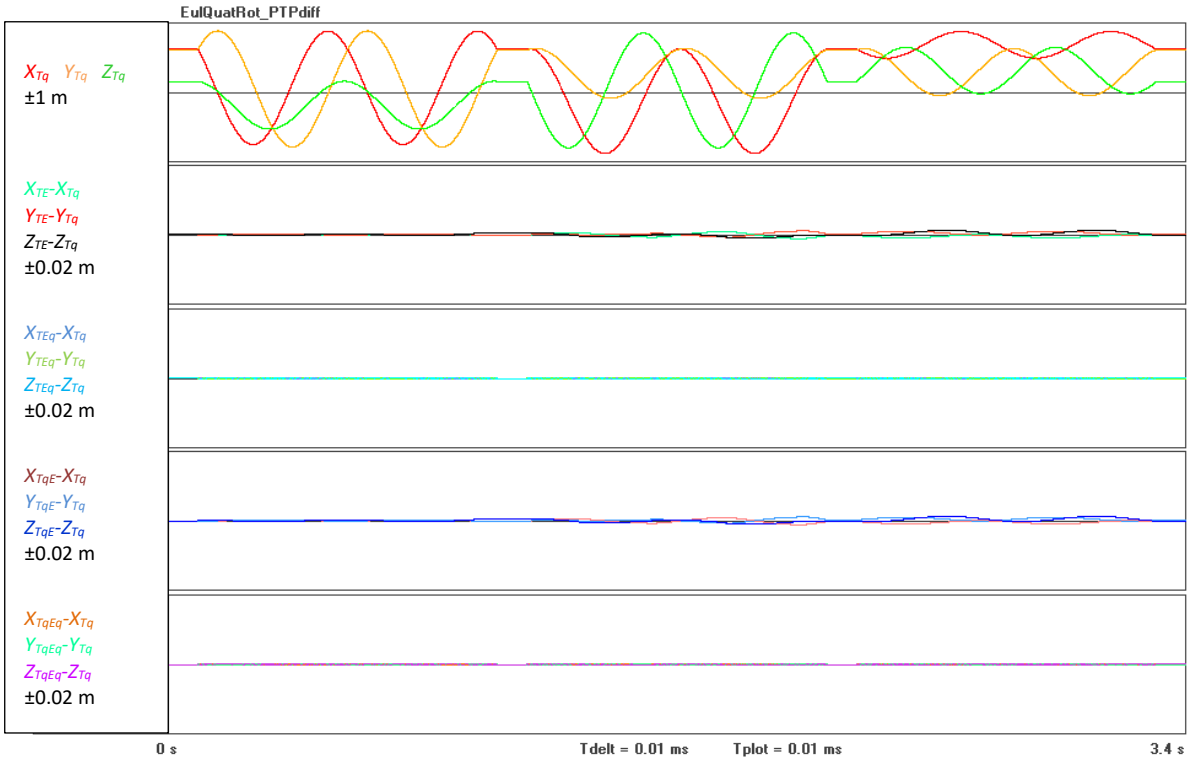

Figure 5. ψ, θ, ϕ configuration with time step = 0.01 ms graphs

ϕ, ψ, θ (inner) Euler configuration and quaternions:

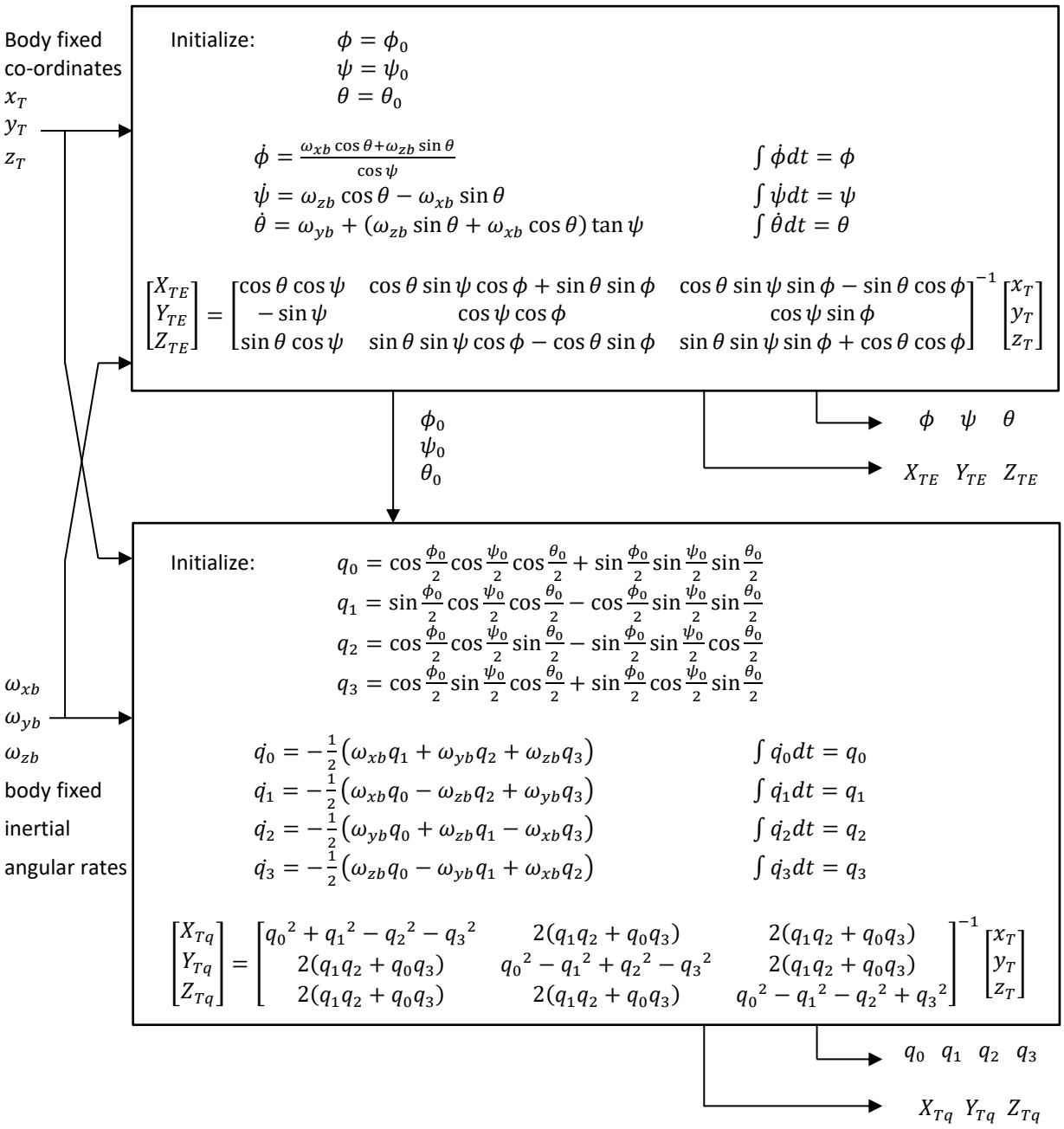

Figure 6. ϕ, ψ, θ (inner) Euler configuration and Quaternion block diagram

The quaternion values are normalised by dividing each value with $\sqrt{{q_0}^2 + {q_1}^2 + {q_2}^2 + {q_3}^2}$ after determining the integrals.

In this configuration Euler angles can be derived from quaternions with the following:

- $\psi_q = \text{asin}[2(q_0q_3 - q_1q_2)]$
- $\phi_q = \text{atan2}\left[\frac{2(q_2q_3 + q_0q_1)/\cos\psi_q}{({q_0}^2 - {q_1}^2 + {q_2}^2 - {q_3}^2)/\cos\psi_q}\right]$
- $\theta_q = \text{atan2}\left[\frac{2(q_1q_3 + q_0q_2)/\cos\psi_q}{({q_0}^2 + {q_1}^2 - {q_2}^2 - {q_3}^2)/\cos\psi_q}\right]$

Although divisions by cosψ_q, as in the last two equations, if negative, causes a 180° difference in the answer, it does not affect the transformation. These divisions may therefore be omitted. These angles may differ from the Euler angles calculated as shown in the top half of the block diagram, but the transformation will still produce the same results. The reason is that the angles will differ such that the components of the transformation matrix, consisting of products depending on the angle values, will stay the same. The ϕ_q, ψ_q, θ_q angles were used to determine a 2nd Euler transformation matrix.

By using the initializing equations for quaternions in the block diagram, two new sets of quaternions were calculated from ϕ, ψ, θ and ϕ_q, ψ_q, θ_q namely $q_{00}, q_{01}, q_{02}, q_{03}$ and $q_{000}, q_{001}, q_{002}, q_{003}$ respectively. These were used to determine 2nd and 3rd quaternion transformation matrices.

The simulation results follow.

Initial settings:

- $x_T = 0.8$ m, $y_T = 0.3$ m, $z_T = -0.2$ m
- $\phi = -0.4$ rad, $\psi = 0.4$ rad, $\theta = 0.0$ rad, (must be set to 0.0 for ψ to travel through 90°, a gimbal lock position)

Again base motions of $2\pi 2.0$ rad/s constant rotational rates were applied as can be seen in the 1st set of 3 graphs in Figure 7. The 3 Euler angles, mostly ramps, follow thereafter, followed by the Euler angles derived from the quaternions. Then follow the 3 sets of quaternions, drawn on slightly different scales (±1, ±1.1, ±1.2) so that they do not cover one another in the time slots where they are the same. Lastly the inertial co-ordinates of the chosen point in the body are drawn, the 1st set (X_{qT}, Y_{Tq}, Z_{Tq}) by using the original quaternions for the transformation, and the 2nd set (X_{TE}, Y_{TE}, Z_{TE}) by using the original Euler angles for the transformation. These two sets are quite the same over the period drawn. No problems were experienced when ψ went through the 90° gimbal lock position, again because the coding of the simulation was done such that the exact singularity point was avoided.

PPT in the titles of the graphs below denotes the Phi-Psi-Theta Euler configuration.

Note the difference in ψ and ψ_q in Figure 7, as well as the differences in the same *q*-parameters. Despite of these differences (X_{Tq}, Y_{Tq}, Z_{Tq}) and (X_{TE}, Y_{TE}, Z_{TE}) are quite the same.

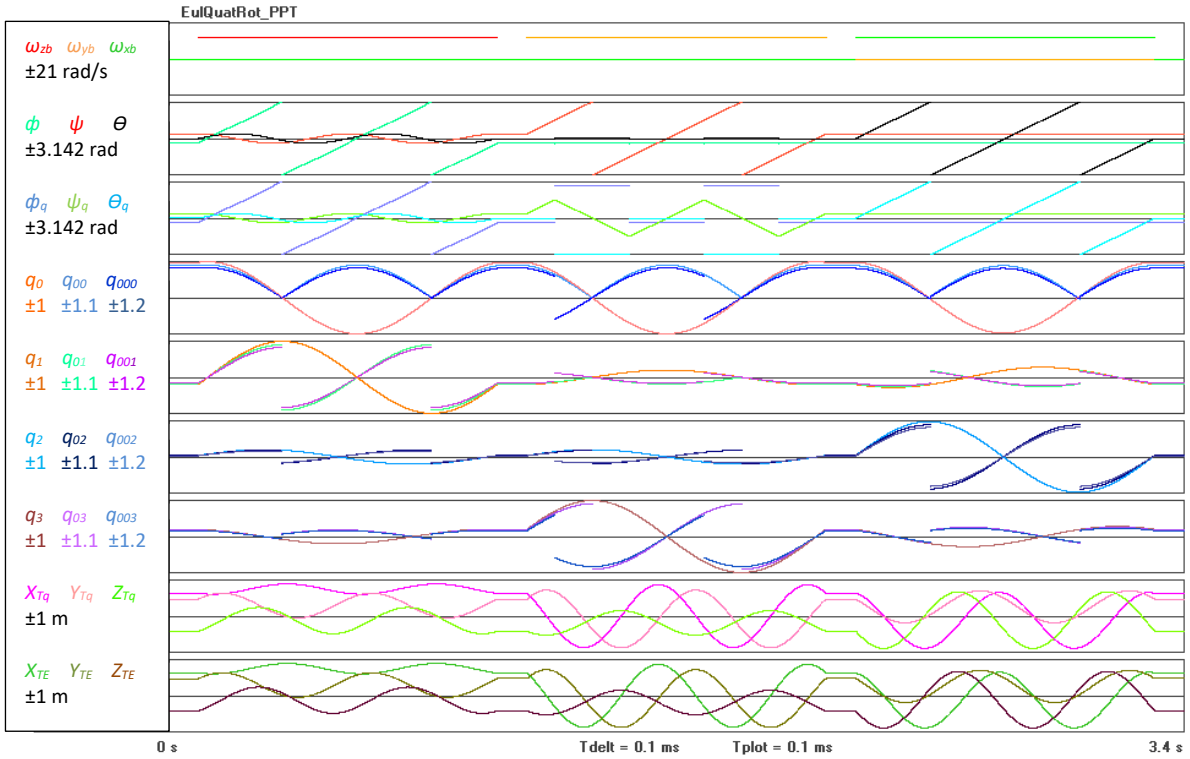

Figure 7. ϕ, ψ, θ configuration with initial $\theta = 0.0$ graphs

The next simulation was done similar to the previous one, except that the initial θ was changed from 0.0 to -0.1 rad. The changes in ϕ, ψ and θ are noteworthy compared to the previous graphs, but the general results are the same as before. The two sets of inertial co-ordinates are still quite the same – compare (X_{TE}, Y_{TE}, Z_{TE}) in Figures 7 and 8.

Note the differences in the same q-parameters in Figure 8. Despite of these differences (X_{Tq}, Y_{Tq}, Z_{Tq}) and (X_{TE}, Y_{TE}, Z_{TE}) are quite the same.

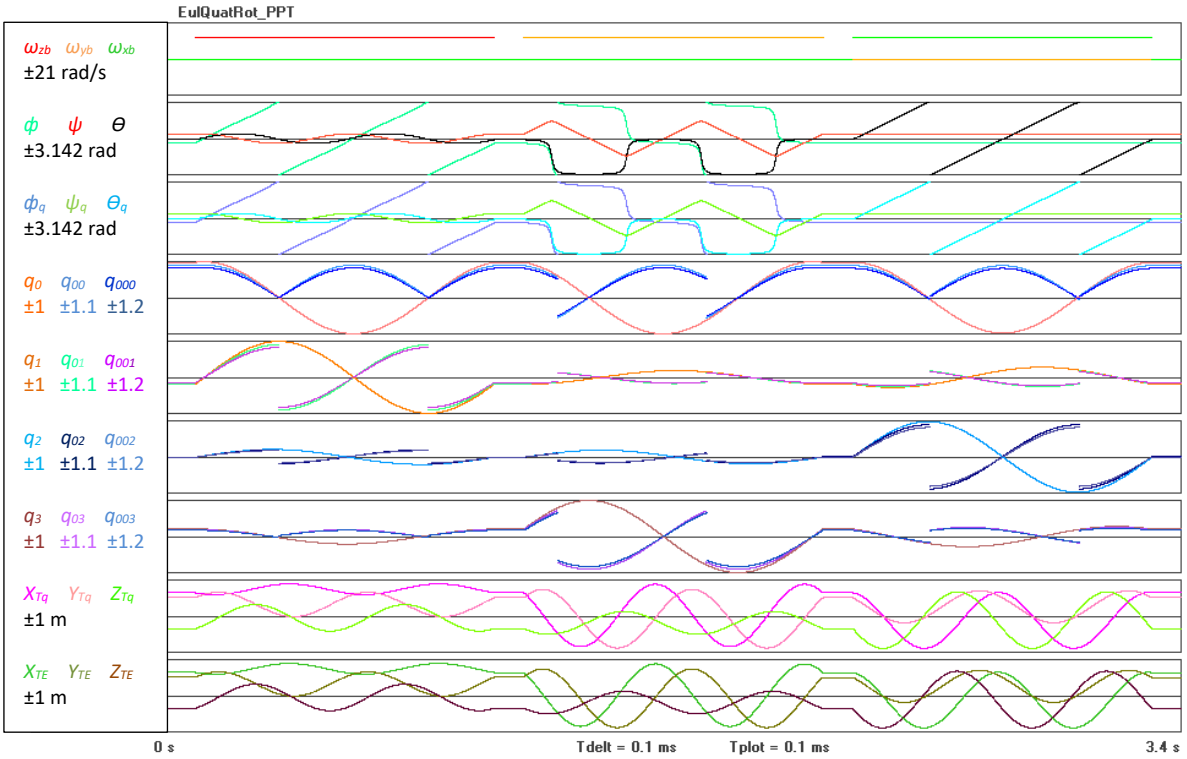

Figure 8. ϕ, ψ, θ configuration with initial $\theta = -0.1$ graphs

The set-up for the next two graphs is the same as the previous simulation; only different signals are plotted. Although the two sets of inertial co-ordinates appeared to be the same before, when plotting their differences on a more sensitive scale, it can be seen that they differ. These differences were also plotted for the transformations done with the other Euler angles and quaternions.

X_{Tq}, Y_{Tq}, Z_{Tq} are the co-ordinates, transformed with the quaternion matrix from quaternion equations.

X_{TE}, Y_{TE}, Z_{TE} are the co-ordinates, transformed with the Euler matrix from the gimbal equations.

X_{TEq}, Y_{TEq}, Z_{TEq} are the co-ordinates, transformed with the Euler matrix derived from quaternion equations.

X_{TqE}, Y_{TqE}, Z_{TqE} are the co-ordinates, transformed with the quaternion matrix derived from the gimbal equations.

X_{TqEq}, Y_{TqEq}, Z_{TqEq} are the co-ordinates, transformed with the quaternion matrix derived from Euler angles derived from quaternion equations.

In the next graphs it is clear that the transformations based on the original Euler angles, in other words the gimbal equations were used, are not very accurate. They are the 2nd and the 4th sets of 3 graphs in Figure 9. It can be solved by performing the simulation at a much smaller incremental time step, which is not necessary for the transformations based on the original quaternions.

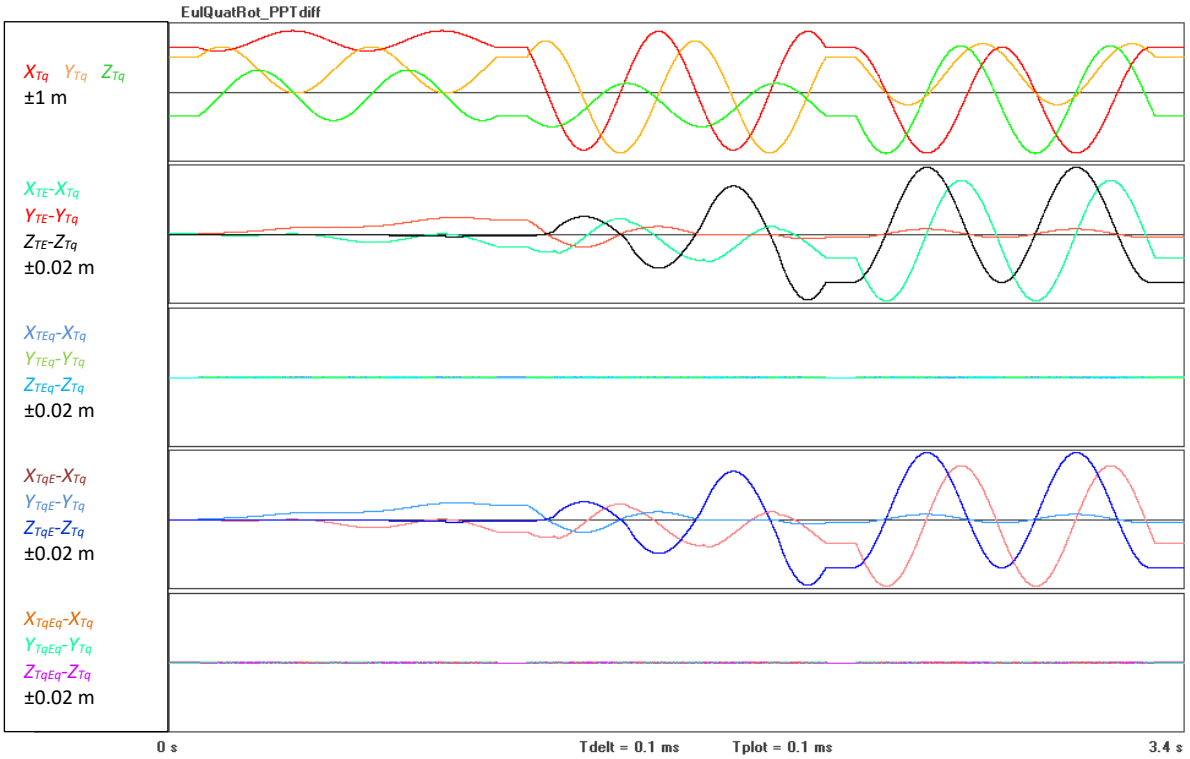

Figure 9. ϕ, ψ, θ configuration with time step = 0.1 ms graphs

Figure 10 shows that a 10 times smaller incremental time step improves the transformations based on the gimbal equations significantly, but a smaller time step is not required for transformations based on the original quaternions. This is strong indication that transformations based on quaternions are preferable.

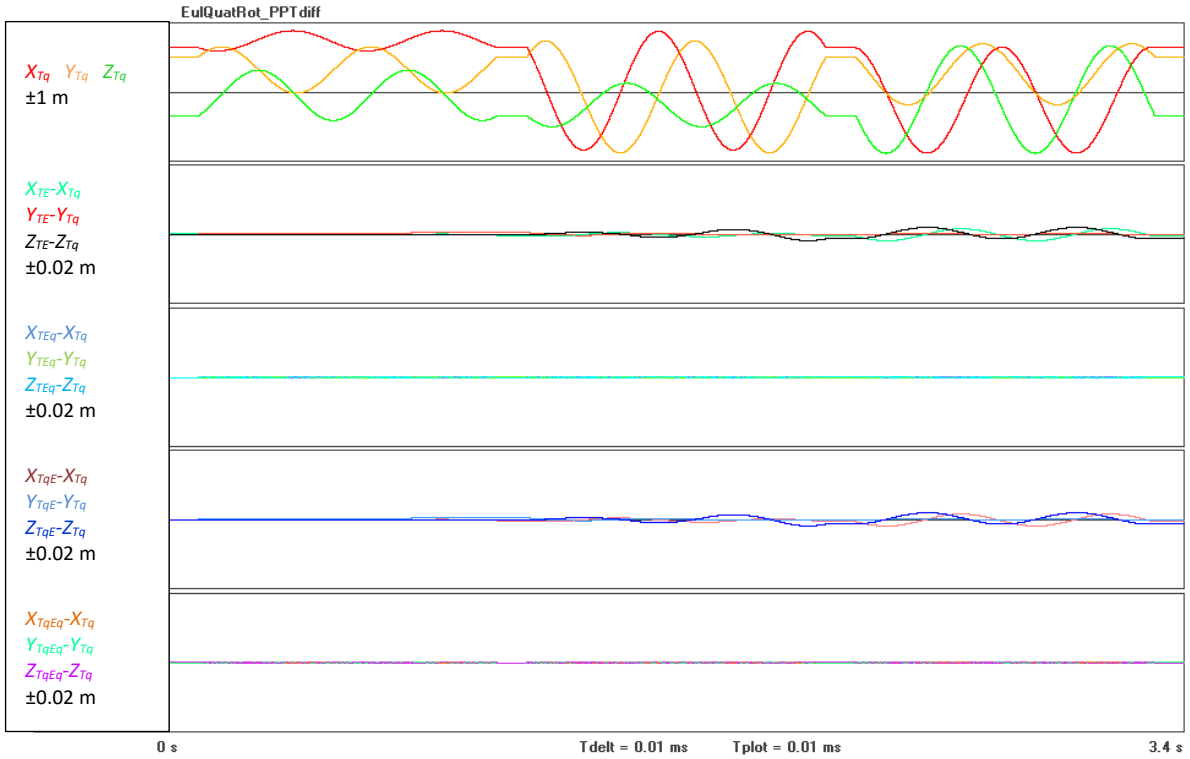

Figure 10. ϕ, ψ, θ configuration with time step = 0.01 ms graphs

Conclusions:

Five transformation matrices for each of two gimbal orientations were evaluated in this paper. They were:

1. The matrix based on original quaternions
2. The matrix based on original Euler angles; it started with the gimbal equations
3. The matrix based on Euler angles derived from the original quaternions
4. The matrix based on quaternions derived from the original Euler angles; it started with gimbal equations
5. The matrix based on quaternions derived from Euler angles derived from the original quaternions

The matrices that used the gimbal equations were found to require much smaller incremental time steps in simulations to give accurate results. Quaternion based transformation matrices are thus superior since fast execution time and accuracy may be important. Since less calculations are required, the 1st transformation is concluded to be the best.

Euler representations did not give gimbal lock problems even though some rotations applied were chosen to let the body rotate through these positions. This was overcome by special coding which is not required for quaternion-based transformation matrices, which is another advantage of quaternions.

Both Euler angle and quaternion values can differ significantly when calculated with the different methods mentioned above. These differences do not cause changes in the transformation results because the values differ such that the transformation matrix components stay the same.

References:

[1] Brian L. Stevens, Frank L. Lewis, Aircraft Control and Simulation, 2nd edition, John Wiley & Sons, Inc., 2003. ISBN-13: 978-0471371458. ISBN-10: 0471371459.

[2] Ken Shoemake, Animating Rotation with Quaternion Curves, The Singer Company, 1985.

[3] E. T. Whittaker, A Treatise on the Analytical Dynamics of Particles & Rigid Bodies, 2nd edition, Cambridge University Press, 1917.

[4] Andrea Alaimo, V. Artale, C. Milazzo & Angela Ricciardello, Comparison between Euler and Quaternion Parametrization in UAV Dynamics. AIP Conference Proceedings, 2013, 1558. 1228-1231. 10.1063/1.4825732.

[5] A. F. L. Bredenkamp, Development and Control of a 3-axis Stabilised Platform. Masters dissertation, University of Stellenbosch, 2007.